Finite-element analysis of a shielded pulsed-current induction heater

Experimental validation of a time-domain thin-shell approach

Ruth V. Sabariego, Peter Sergeant, Johan Gyselinck, Patrick Dular, Luc Dupré and Christophe Geuzaine
(Affiliations are shown at the end of the article.)

Abstract

Purpose – The aim of this paper is the experimental validation of an original time-domain thin-shell formulation. The numerical results of a three-dimensional thin-shell model are compared with the measurements performed on a heating device at different working frequencies.

Design/methodology/approach – A time-domain extension of the classical frequency-domain thin-shell approach is used for the finite-element analysis of a shielded pulse-current induction heater. The time-domain interface conditions at the shell surface are expressed in terms of the average flux density vector in the shell, as well as in terms of a limited number of higher-order components.

Findings – A very good agreement between measurements and simulations is observed. A clear advantage of the proposed thin-shell approach is that the mesh of the computation domain does not depend on the working frequency anymore. It provides a good compromise between computational cost and accuracy. Indeed, adding a sufficient number of induction components, a very high accuracy can be achieved.

Originality/value – The method is based on the coupling of a time-domain 1D thin-shell model with a magnetic vector potential formulation via the surface integral term. A limited number of additional unknowns for the magnetic flux density are incorporated on the shell boundary.

Keywords Electromagnetism, Finite-element methods, Electric motors, Heaters

Paper type Research paper

1. Introduction

Conducting pieces can be thermally treated by means of induction heaters that generate strong alternating magnetic fields and induce eddy currents in them. Traditionally, the current source of these heating devices was sinusoidal. However, the use of pulsed currents becomes a very attractive alternative thanks to several interesting technological effects. Specifically, it allows to reduce the inductor dimensions and to achieve a more uniform heating (Shenkman *et al.*, 2006).

The shielding of these devices is often crucial to mitigate the magnetic field in its environment and reduces the hazardous exposure of both the human operator and the electronic equipment. In practice, these shields are thin metallic sheets with holes to

This work is partly supported by the Belgian Science Policy (IAP P6/21) and the Walloon Region.

guarantee the accessibility to the heater (to guide control or power wires, to allow cooling [...]). Their numerical modeling becomes thus an essentially 3D task.

The finite element (FE) analysis of these magnetic shielding problems involving thin shells may suffer from both meshing difficulties and high-computational cost. The well-known thin-shell approach allows to overcome these drawbacks, but it is most often restricted to linear and time-harmonic analyses (Krähenbühl and Muller, 1993; Mayergoyz and Bedrosian, 1995; Geuzaine *et al.*, 2000).

Considering a pulsed current as heating source demands a time-domain model. In (Gyselinck *et al.*, 2008) a pure time-domain approach with the magnetic vector potential formulation is proposed. It is based on the use of orthogonal polynomial basis functions to account for the variation of the magnetic flux through the shell thickness. The method is further extended to the magnetic field formulation in (Sabariego *et al.*, 2008).

This paper deals with the analysis of a shielded induction heater with a pulsed current. Numerical results obtained with a time-domain thin-shell approach are compared with measurements performed on an experimental setup.

2. Magnetodynamic formulation

We consider a magnetodynamic problem in a bounded domain $\Omega = \Omega_c \cup \Omega_c^C \in \mathbb{R}^3$ with boundary Γ. The conductive and non-conductive parts of Ω are denoted by Ω_c and Ω_c^C. Source inductors constitute domain $\Omega_i \subset \Omega_c^C$ (Figure 1).

The Maxwell equations and constitutive laws governing the low-frequency eddy-current problems are:

$$\text{curl } h = j, \text{div } b = 0, \text{curl } e = -\partial_t b, b = \mu h, j = \sigma e, \tag{1a–e}$$

where h is the magnetic field, b the magnetic flux density (or induction), e the electric field, j the electric current density, μ the permeability (reluctivity $\nu = 1/\mu$) and σ the conductivity (resistivity $\rho = 1/\sigma$).

The a-formulation is obtained from the weak form of the Ampère law (1a):

$$(\nu \text{curl } a, \text{curl } a')_\Omega + (\sigma \partial_t a, a')_{\Omega_c} + \langle n \times h, a' \rangle_\Gamma = (j_i, a')_{\Omega_i}, \tag{2}$$

where a is the magnetic vector potential, n is the outward unit normal vector on Γ, j_i is a prescribed current density, $(\cdot,\cdot)_\Omega$ and $\langle \cdot,\cdot \rangle_\Gamma$ denote a volume integral in Ω and a surface integral on Γ of the scalar product of their arguments.

The first step in the thin-shell approach consists in reducing the thin-shell volume $\Omega_s \subset \Omega_c$ (thickness d) to an average surface Γ_s situated halfway between the inner surface Γ_s^- and outer surface Γ_s^+ of Ω_s (outward normal n_s), as shown in Figure 1. Next the surface integral in equation (2) is modified on the basis of the 1D thin-shell model described hereafter.

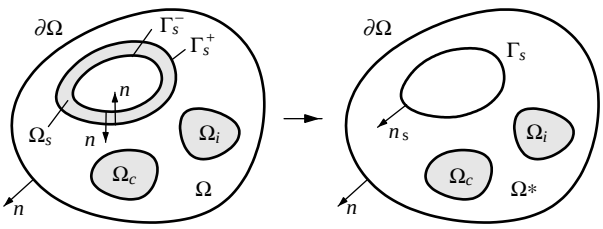

Figure 1.
Bounded domain Ω and reduction of the thin-shell volume Ω_s to the surface Γ_s

3. 1D thin-shell model

We adopt a local coordinate system *xyz* with the *z*-axis normal to the shell (i.e. parallel to n_s) and $z = 0$ at its center. In the 1D model of the shell, only the variation of the magnetic field $h(z,t)$ and the magnetic induction $b(z,t)$ tangential to the boundary of the shell Γ_s is considered throughout the shell thickness. The tangential components of the magnetic field h on Γ_s^+ and Γ_s^- (both sides of the shell) are defined as:

$$h_t^+ = n_s \times (h|_{\Gamma_s}^+ \times n_s), \quad h_t^- = n_s \times (h|_{\Gamma_s}^- \times n_s). \tag{3a, b}$$

Analogously to equation (3), hereafter f_t denotes the tangential component of a field f on a surface Γ with normal n.

A. Governing differential equation

The 1D eddy-current problem in the shell ($-d/2 \leq z \leq d/2$) is governed by:

$$\partial_z^2 h_t(z,t) = \sigma \partial_t b_t(z,t), \tag{4}$$

with constitutive law $h_t(z,t) = \nu b_t(z,t)$. The associated boundary conditions on the upper (+) and lower (−) surfaces of the shell are given by $h_t^{\pm}(t) = h_t(\pm d/2, t)$.

B. Harmonic case

For a sinusoidal time variation at pulsation ω, we define the relative shell thickness as d/δ, with $\delta = 1/\sqrt{2/\sigma\mu\omega}$ the penetration depth.

In case of constant permeability, the diffusion equation (4) can be solved analytically, which leads to an expression in terms of the complex representation (symbols in bold) of $h_t^+(t)$, $h_t^-(t)$ and $b_0(t)$ (Krähenbühl and Muller, 1993):

$$\boldsymbol{h}_t^+ + \boldsymbol{h}_t^- = 2\nu \mathrm{Y}\left(\frac{d}{\delta}\right)\mathbf{b}_0, \tag{5}$$

with:

$$\boldsymbol{Y}\left(\frac{d}{\delta}\right) = \frac{1+\boldsymbol{i}}{2}\left(\frac{d}{\delta}\right)\ \mathrm{cotanh}\left(\frac{1+\boldsymbol{i}}{2}\frac{d}{\delta}\right),$$

where $\boldsymbol{i}$ is the imaginary unit.

The well-known FE frequency-domain approach includes the 1D thin-shell model in a 2D and 3D analysis via the tangential fields h_t^+, h_t^- and equation (5) as done in Krähenbühl and Muller (19930, Mayergoyz and Bedrosian (1995), and Geuzaine *et al.* (2000).

C. Time-domain extension

We now develop a time-domain extension of equation (5) by considering $n + 1$ polynomial basis functions for the expansion of the tangential induction $b_t(z,t)$ (Gyselinck *et al.*, 2008; Sabariego *et al.*, 2008). We choose a set of orthogonal Legendre polynomials $\alpha_k(z)$ to expand $b_t(z,t)$, i.e.:

$$b_t(z,t) = \sum\nolimits_{k=0}^{n} \alpha_k(z) b_k(t), \tag{6}$$

with $|\alpha_k(\pm d/2)| = 1$.

Strongly satisfying equation (4), the magnetic field $h_t(z,t)$ can be written as:

$$h_t(z,t) = \frac{h_t^+(t) + h_t^-(t)}{2} + \frac{h_t^+(t) - h_t^-(t)}{d}\ z + \sigma d^2 \sum_{k=0}^{n}\ \beta_k(z)\partial_t b_k(t), \tag{7}$$

where $d^2\partial_z^2\beta_k = \alpha_k(z)$ and $\beta_k(\pm d/2) = 0$.

Next, with a finite number of basis functions, the constitutive law $h(z,t) = \nu b(z,t)$ can be weakly imposed as:

$$\int_{-d/2}^{d/2} \alpha_k(z)\big(h_t(z,t) - \nu b_t(z,t)\big)\mathrm{d}z = 0, \tag{8}$$

which leads to $n+1$ differential equations ($k = 0,\ldots,n$) in terms of $b_0(t),\ldots,b_n(t)$, $h_t^+(t)$ and $h_t^-(t)$ (Gyselinck *et al.*, 2008; Sabariego *et al.*, 2008).

The following system of linear differential equations is obtained:

$$[H(t)] = \nu[P][B(t)] + \sigma d^2[Q]\partial_t[B(t)], \tag{9}$$

with $[H(t)] = \left[\frac{h_t^+ + h_t^-}{2}\ \frac{h_t^+ - h_t^-}{6} 0\ldots 0\right]^T$ and $[B(t)] = [b_0(t)b_1(t)\ldots b_n(t)]^T$. The elements p_k and q_{kl} ($k,l = 0,\ldots,n$) of the diagonal matrix $[P]$ and triangular matrix $[Q]$ are given by:

$$p_k = \int_{-d/2}^{d/2} \alpha_k(z)\alpha_k(z)\mathrm{d}z,\ \ q_{k,l} = \int_{-d/2}^{d/2} \alpha_k(z)\beta_l(z)\mathrm{d}z. \tag{10}$$

4. FE implementation

In the thin-shell formulation, the thin-shell volume Ω_s is excluded from the original calculation domain Ω. Further, the surface Γ_s with outward normal n_s and situated halfway between the inner surface Γ_s^- and outer surface Γ_s^+ of Ω_s is added to the new domain $\Omega\backslash\Omega_s$ (Figure 1). In order to account for the changes in these domains, the surface integral term in equation (2) is modified (Gyselinck *et al.*, 2008; Sabariego *et al.*, 2008). The new weak form reads:

$$\begin{aligned}(\nu\ \mathrm{curl}\ a, \mathrm{curl}\ a')_{\Omega\backslash\Omega_s} + (\sigma\partial_t a, a')_{\Omega_c} + \langle n\times h, a'\rangle_{\Gamma} \\ + \langle n_s\times h, a'\rangle_{\Gamma_s^-} - \langle n_s\times h, a'\rangle_{\Gamma_s^+} = (j_i, a')_{\Omega_i}.\end{aligned} \tag{11}$$

The time-domain behavior of the thin shell is taken into account by introducing the tangential vector fields $b_0, b_1,\ldots,b_n$ on Γ_s as unknowns.

Taking into account the boundary conditions $h_t^{\pm}(t) = h_t(\pm d/2, t)$ in the 1D eddy-current problem and the Ampère law (1a), the tangential component of the magnetic field h_t is discontinuous across Γ_s and related to the net current dj_0 in the shell as:

$$h_t^+ - h_t^- = -n_s \times d\, j_0(t), \tag{12}$$

with $j_0(t)$ the average current density vector tangential to Γ_s. Moreover, the tangential component of the magnetic vector potential a_t is also discontinuous across Γ_s and is related to the net flux db_0 in the shell as:

$$a_t^+ - a_t^- = -n_s \times d\, b_0(t), \tag{13}$$

with $b_0(t)$ the average flux density vector tangential to Γ_s.

We therefore decompose a as $a_c + a_d$, the tangential components of a_c and a_d being continuous and discontinuous across the shell, respectively.

Without loss of generality we can choose a_d to be zero in the volume enclosed by Γ_s. Furthermore, conformity can be ensured by limiting its support to one layer of elements touching Γ_s^+ (Geuzaine *et al.*, 2000). By considering $a^- = a_c$ and $a_d = -n_s \times db_0$ together with equation (12), we can work out the two new surface terms in equation (2). They are given by:

$$\begin{aligned}\langle n_s \times h, a' \rangle_{\Gamma_s^-} - \langle n_s \times h, a' \rangle_{\Gamma_s^+} \\ = -\langle n_s \times h_t^+, a_c' \rangle_{\Gamma_s} - \langle n_s \times h_t^+, a_d' \rangle_{\Gamma_s} + \langle n_s \times h_t^-, a_c' \rangle_{\Gamma_s} \\ = d\langle h_t^+, b_0' \rangle_{\Gamma_s} - d\langle j_0, a_c' \rangle_{\Gamma_s}.\end{aligned} \tag{14}$$

From the first two lines of system (9) we get an expression for h_t^+ and h_t^- in terms of b_0, b_1, b_2 and b_3 (assuming $n \geq 2$):

$$h_t^{\pm} = \nu b_0 + \sigma d^2 (q_{00} \partial_t b_0 + q_{02} \partial_t b_2) \pm 3\nu b_1 \pm 3\sigma d^2 (q_{01} \partial_t b_1 + q_{03} \partial_t b_3). \tag{15}$$

The weak form (11) is thus coupled with the time-domain thin-shell approximation via a_c, a_d in $\Omega \backslash \Omega_s$ and b_0, b_1, b_2 and b_3 on Γ_s.

Next, from equations (12) and (7), we get the second condition concerning the tangential components $a_{c,t}$ and $a_{d,t}$ of a_c and a_d. We have:

$$\frac{-\sigma \partial_t (2a_{c,t} + a_{d,t})}{2} = \frac{2}{d} \nu b_1 + \sigma d \left(\frac{1}{5} \partial_t b_1 - \frac{1}{70} \partial_t b_3 \right), \tag{16}$$

which we can weakly impose on Γ_s with test functions b_1' and b_3'.

The remaining equations of system (9) result in the following weak forms with test functions b_l' ($l = 2,3,\ldots,n$):

$$0 = \langle \nu p_l b_l, b_l' \rangle_{\Gamma_s} + \sum_{i=-2,0,2} \langle \sigma d^2 q_{l,l+i} \partial_t b_{l+i}, b_l' \rangle_{\Gamma_s}. \tag{17}$$

5. Analysis of the induction heater

The induction heater comprises a pulsed-current excitation coil and a cylindrical shield (190-mm high), made either of copper (0.5-mm width, $\sigma = 5.3\ 10^7$ S/m) or steel (0.65-mm width, $\sigma = 5.9\ 10^6$ S/m, $\mu_r = 372$). The steel shield has circular perforations of 76-mm diameter; two holes aligned in the axial direction and repeated periodically along the circumference. The distance between the holes in the axial and azimuthal directions is approximately the same. The workpiece is a cylindrical aluminium plate (radius $= 191$ mm, height $= 10$ mm, $\sigma = 3.7\ 10^7$ S/m, $\mu_r = 1$). The induction-heating setup is shown in Figure 2.

Although the current waveforms in a pulsed induction heater are usually generated by a power electronic converter, our experimental setup (Figure 3) is fed by a linear amplifier. The amplitude of the current is about ten times smaller than in the induction-heating device in (Shenkman *et al.*, 2006), but the results can be scaled because our setup does not contain nonlinear materials whose electromagnetic properties (such as permeability) change with the field amplitude.

The generation of the waveform signals for the linear amplifier was done by a National Instruments PCI-6110 card, controlled by LabVIEW. The pulsed-current waveform, generated for a given frequency and peak current, is programmed based on the analytical expression found in Shenkman *et al.* (2006) and consists of three parts: part 1 where a capacitor is charged (load current is zero); part 2 where the capacitor is discharged (load current increases and reaches maximum; and part 3 where the capacitor is short circuited (load current decreases to zero). The output of the linear amplifier differs from the input waveform especially for the highest considered frequency, due to the limited slew rate of the amplifier (Figure 3). Note that the three curves in Figure 3 are not in phase due to the lack of triggering when measuring. This phase displacement could be easily avoided though it would not influence the quality of the results.

The current waveform and the magnetic induction waveform were measured with a Tektronix current probe and an inductive magnetic field sensor, respectively. Both signals were sampled simultaneously at 500 samples per period, resulting in a maximal sample rate of 5 MS/s at 10 kHz. Measurements were carried out with the excitation coil working at three different frequencies 100 Hz, 1 and 10 kHz and in the presence of the aluminum plate for the following situations: with no shield; with an axisymmetric copper shield; and with a perforated shield in steel (Figure 2). In all considered cases, the measured and computed vertical components of the magnetic flux density b are compared at a point outside the shield in the symmetry plane (50 cm from the center of the device and 20 cm from the shield position). The time-domain thin-shell approach is applied to model the shield.

Time-stepping simulations with imposed measured pulsed current at three different frequencies $f = 100$ Hz, 1 and 10 kHz are carried out. A period $T = 1/f$ is time stepped

Figure 2.
Picture of the studied induction-heating application (left); sketch of the setup (right)

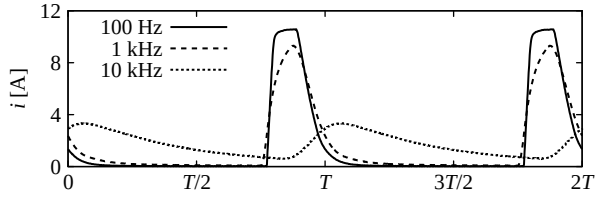

Notes: f = 100Hz, 1;10kHz (period $T = 1/f$)

Figure 3.
Measured pulsed current at different frequencies

with $\Delta t = T/120$. Two periods of the simulation results in steady state are compared with the performed measurements.

In order to have an idea of quality of the measurements, we consider first the case with no shield. An excellent agreement is shown in Figure 4.

Then a copper shield is added to the setup. The thin-shell approach is applied to the shield in an axisymmetric model. Results are shown in Figure 5. The measurements are quite noisy at 1 and 10 kHz due to the small amplitude variation of the magnetic field outside the shield. At all considered frequencies, there is hardly any skin effect (uniform distribution of the eddy currents), so that the thin-shell method gives a good approximation with $n = 0$ (only two additional unknowns on Γ_s: b_0 and b_1). Indeed, the difference between results for $n = 0$ and $n = 2$ at 1 and 10 kHz is negligible.

Eventually, the perforated steel shield shown in Figure 2 is studied. A full 3D FE model is used (see detail of the 3D mesh in Figure 6). The nonlinearity of the steel is not

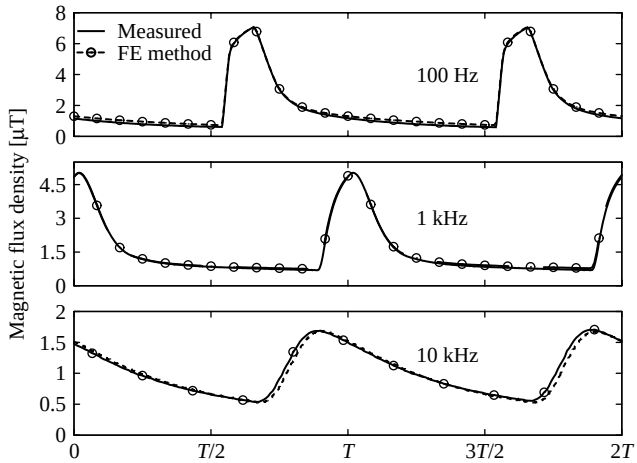

Figure 4.
Vertical component of magnetic flux density at a distance of 50 cm from the center of the induction heater, no shield considered

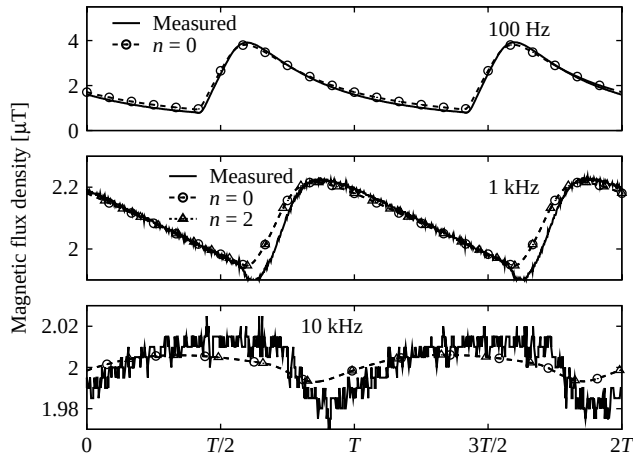

Figure 5.
Vertical component of magnetic flux density at a distance of 50 cm from the center of the induction heater and outside a cylindrical copper shield

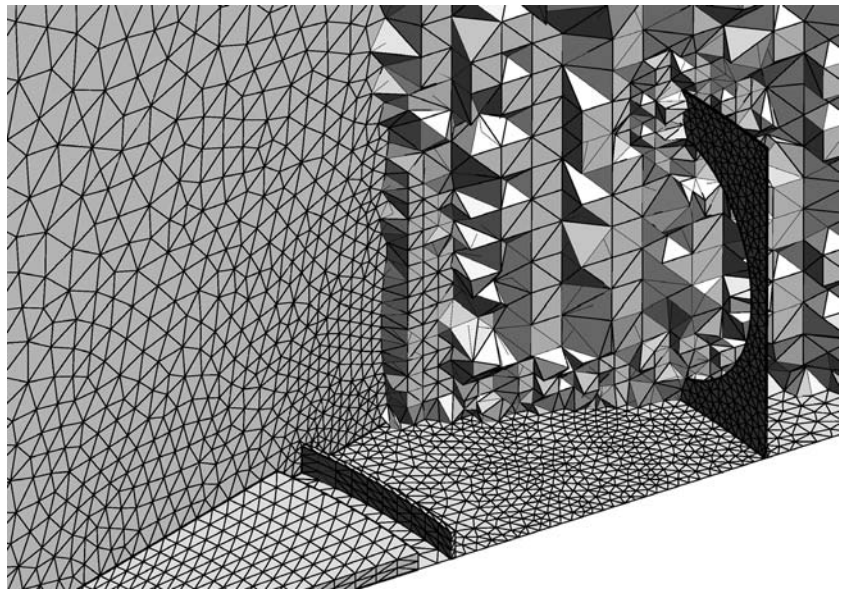

Figure 6.
Detail of the 3D mesh

taken into account in the simulations but is proved to be negligible by the results hereafter. Indeed, the fields in the shield are weak enough (reduced power) to assume a constant permeability. At 100 Hz, there is hardly any skin effect, and thin-shell approximation is already excellent with $n = 0$. At 10 kHz, the skin effect is much more important. The thin-shell approach with $n = 2$ (additional unknowns on Γ_s: b_0, b_1, b_2 and b_3) gives a good agreement with measurements. The numerical model shows thus a very good correlation with the measurements.

A. Computational cost

In order to highlight the interest of the proposed thin-shell method, we analyse the computational data for the induction heater shielded with a perforated steel layer. The system of algebraic equations is solved by means of an LU solver on a MacBook Pro with a 2.4 GHz Intel Core 2 Duo Processor.

The 3D FE models employ a mesh (Figure 6) that yields N complex unknowns. In the conventional FE method, this value N increases with the number of layers along the shield thickness used for discretising it, what depends in turn on the working frequency (the higher the frequency, the higher the number of required layers). Besides the huge difference between the width of the shield and its other dimensions makes the meshing task considerably arduous. With the thin-shell approach, the shield is modeled by a surface and the mesh remains the same for all considered frequencies, which is the main advantage of the method. N augments with a fix and reduced number of complex unknowns when increasing n (e.g. 1,279 new unknowns for a unitary increment and the mesh considered in Table I).

Let us analyse an example shown in Table I. At 10 kHz, a number of four layers was required for ensuring good results with the conventional 3D FE method. When using

the thin-shell approach the reduction in computational is 28 percent for $n = 0$, 21 percent for $n = 2$, 17 percent for $n = 4$ and there is no gain for $n = 6$. For the problem at hand, the accuracy of the approximation is high enough with $n = 2$. We would only need to increase n for higher frequencies, and in that case the number of layers in the conventional model should also be increased. See Table I and Figure 7 for further results.

6. Conclusions

A time-domain finite-element method for the analysis of thin-shells has been validated with measurements. The method is based on the coupling of a time-domain 1D thin-shell model with a magnetic vector potential formulation via the surface integral term. A limited number of additional unknowns for the magnetic flux density are incorporated on the shell boundary.

A very good agreement between measurements and simulations is observed. A clear advantage of the proposed thin-shell approach is that the mesh of the computation domain does not depend on the working frequency anymore. It provides a good compromise between computational cost and accuracy. Indeed, adding a sufficiently high number of induction components, a very high accuracy can be achieved.

	3D FE model			Thin-shell approach	
Layers	N	t(s)	n	N	t(s)
2	71,384	35	0	65,589	30
4	74,266	42	2	68,147	33
6	85,098	54	4	70,705	35
8	91,466	63	6	73,263	42
10	97,747	66			

Table I.
Computation time (per time step) for the conventional FE method and the thin-shell approach

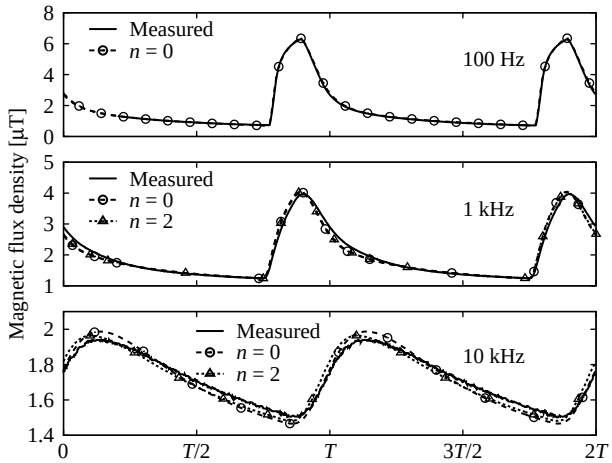

Figure 7.
Vertical component of magnetic flux density at a distance of 50 cm from the center of the induction heater and outside a perforated steel shield

References

Geuzaine, C., Dular, P. and Legros, W. (2000), "Dual formulations for the modeling of thin electromagnetic shells using edge elements", *IEEE Trans. Magn.*, Vol. 36 No. 4, pp. 799-803.

Gyselinck, J., Sabariego, R.V., Dular, P. and Geuzaine, C. (2008), "Time-domain finite-element modelling of thin electromagnetic shells", *IEEE Trans. Magn.*, Vol. 44 No. 6, pp. 742-5.

Krähenbühl, L. and Muller, D. (1993), "Thin layers in electrical engineering. Example of shell models in analyzing eddy-currents by boundary and finite element methods", *IEEE Trans. Magn.*, Vol. 29 No. 5, pp. 1450-5.

Mayergoyz, I.D. and Bedrosian, G. (1995), "On calculation of 3D eddy currents in conducting and magnetic shells", *IEEE Trans. Magn.*, Vol. 31 No. 3, pp. 1319-24.

Sabariego, R.V., Geuzaine, C., Dular, P. and Gyselinck, J. (2008), "h- and a- time-domain formulations for the modelling of thin electromagnetic shells", *IET Sci. Meas. Technol.*, Vol. 2 No. 6, pp. 402-8.

Shenkman, A., Berkovich, Y. and Axelrod, B. (2006), "Pulse converter for induction-heating applications", *IEE Proc. Electr. Power Appl.*, Vol. 153 No. 6, pp. 864-72.

Authors' affiliations

Ruth V. Sabariego, Applied and Computational Electromagnetics (ACE), Department of Electrical Engineering and Computer Science (Institut Montefiore), University of Liège, Liège, Belgium.

Peter Sergeant Department of Electrical Energy, Systems and Automation, Ghent University, Ghent, Belgium and Department of Electrotechnology, Faculty of Applied Engineering Sciences, University College Ghent, Ghent, Belgium.

Johan Gyselinck Energy Group, Department of Bio, Electro and Mechanical Systems (BEAMS), Université Libre de Bruxelles (ULB), Brussels, Belgium.

Patrick Dular Applied and Computational Electromagnetics (ACE), Department of Electrical Engineering and Computer Science (Institut Montefiore), University of Liège, Liège, Belgium and Fonds de la Recherche Scientifique, F.R.S.-FNRS, Bruxelles, Belgium.

Luc Dupré, Department of Electrical Energy, Systems and Automation, Ghent University, Ghent, Belgium.

Christophe Geuzaine, Applied and Computational Electromagnetics (ACE), Department of Electrical Engineering and Computer Science (Institut Montefiore), University of Liège, Liège, Belgium.

About the authors

Ruth V. Sabariego graduated in Telecommunication Engineering in 1998 at the University of Vigo, Spain. She received the PhD degree in Applied Sciences from the University of Liège, Belgium, in 2004. From 1998 till 2000, she was a Research Assistant at the Department of Communication Technology, University of Vigo, Spain. In October 2000, she joined the Department of Electrical Engineering and Computer Science, University of Liège, Belgium, where she is now with the Applied and Computational Electromagnetics research group. Her research is situated in the domain of applied mathematics and computational electromagnetics (both low and high frequency). Currently, she devotes special attention to the study and development of computational homogenization techniques for modeling, e.g. modern composites with non-periodic structure. Ruth V. Sabariego is the corresponding author and can be contacted at: r.sabariego@ulg.ac.be

Peter Sergeant was born in 1978. In 2001, he graduated in Electrical and Mechanical Engineering at the Ghent University, Belgium. In 2006, he received the degree of Doctor in Engineering Sciences from the same university. He joined the Department of Electrical Energy,

Systems and Automation, Ghent University in 2001 as Research Assistant. From 2006, he is a Postdoctoral Researcher for the Fund of Scientific Research Flanders (FWO) at Ghent University, and since 2008 also a Researcher at University College Ghent. His main research interests are numerical methods in combination with optimization techniques to design nonlinear electromagnetic systems, in particular electromagnetic actuators and magnetic shields.

Johan Gyselinck graduated in Electromechanical Engineering in 1991 and received the PhD degree in 2000, both at the Ghent University, Belgium. Since 2004, he is an Associate Professor at the ULB, where he teaches electrical machines and drives and power electronics. His past and present research mainly concerns the numerical computation of magnetic fields (mostly using the FE method), the simulation and control of electrical machines and drives, and the design of electrical machines for various applications (servodrives, wind turbine generators, electric traction [...]). He is first the Author and Co-author of some 50 papers in international scientific journals with reviewing committee and over 100 papers in conference proceedings. He is also an active member of the scientific committee and/or reading committee of several international conferences.

Patrick Dular received the Electrical Engineer degree and PhD degree in Applied Science from the University of Liège, Belgium, in 1990 and 1994, respectively. He is currently with Applied and Computational Electromagnetics unit (ACE), Department of Electrical Engineering and Computer Science, University of Liège, as a Senior Research Associate with the Belgian (FRS.-FNRS). His research mainly deals with the numerical modeling of coupled problems in electromagnetic systems, including both physical models and numerical techniques coupling.

Luc Dupré was born in 1966, graduated in Electrical and Mechanical Engineering in 1989 and received the degree of Doctor in Applied Sciences in 1995, both from the Ghent University, Belgium. He joined the Department of Electrical Energy, Systems and Automation, Ghent University in 1989 as a Research Assistant. From 1996 until 2003, he has been a Postdoctoral Researcher for the Fund of Scientific Research-Flanders (FWO). In 2003, he became a research professor and is since 2006 a Full Professor at the Ghent University. His research interests mainly concern numerical methods for electromagnetics, especially in electrical machines and biomedical applications, modeling and characterisation of magnetic materials.

Christophe Geuzaine graduated in Electrical Engineering in 1996 and received the PhD degree in 2001, both at the University of Liège, Belgium. From 2002 to 2005, he has been a Post-Doctoral Scholar at the California Institute of Technology and a Post-Doctoral Fellow with the Belgian FRS-FNRS. In 2005, he became an Assistant Professor in Mathematics at Case Western Reserve University, before joining the faculty at the University of Liège in 2007, where he currently leads the Applied and Computational Electromagnetics research group. Geuzaine has published over 45 articles in international peer-reviewed journals and he has created two widely used open source software tools: the general FE solver GetDP and the well-known mesh generator Gmsh. His research interests encompass modeling, analysis, algorithm development and simulation for problems arising in various areas of engineering and science, with current applications in computational electromagnetism and biomedical problems.